

Flip of spin helix chirality and ferromagnetic state in $\text{Fe}_{1-x}\text{Co}_x\text{Ge}$ compounds

S. V. Grigoriev,^{1,2} S.-A. Siegfried,³ E. V. Altynbayev,^{1,2} N. M. Potapova,¹ V. Dyadkin,^{1,4} E. V. Moskvina,^{1,2} D. Menzel,⁵ A. Heinemann,³ S. N. Axenov,⁶ L. N. Fomicheva,⁷ and A. V. Tsvyashchenko^{7,8}

¹*Petersburg Nuclear Physics Institute, RNC “Kurchatov institute”, Gatchina, St-Petersburg, 188300, Russia*

²*Saint-Petersburg State University, Ulyanovskaya 1, Saint-Petersburg, 198504, Russia*

³*Helmholtz Zentrum Geesthacht, Geesthacht, 21502, Germany*

⁴*Norwegian Beamlines at the European Synchrotron Radiation Facility, Grenoble, 38000 France*

⁵*Institut für Physik der Kondensierten Materie, TU Braunschweig, 38106 Braunschweig, Germany*

⁶*Institute for Nuclear Research, Russian Academy of Sciences, 117312 Moscow, Russia*

⁷*Institute for High Pressure Physics, Russian Academy of Sciences, 142190 Troitsk, Moscow, Russia*

⁸*Skobel'syn Institute of Nuclear Physics, Moscow State University, 119991 Moscow, Russia*

(Received 27 August 2013; revised manuscript received 11 October 2014; published 13 November 2014)

We have synthesized the solid solutions of $\text{Fe}_{1-x}\text{Co}_x\text{Ge}$ compounds with x running from 0.0 to 0.9. Small-angle neutron scattering and magnetization measurements have shown that these compounds are ordered into the spin helix structure below the critical temperature T_c . The helix is transformed into the ferromagnet by application of the magnetic field above the critical value H_{c2} . It is shown that T_c decreases smoothly with concentration x from 280 K for FeGe to 0 for CoGe. The values of the helix wave vector k_s and the critical field H_{c2} depend strongly on concentration x , firstly, decreasing from pure FeGe to its minimum ($|\mathbf{k}_s| \rightarrow 0$, $H_{c2} \rightarrow 0$) at $x_c \approx 0.6$, and, then increasing again at higher x . Thus, we observe a transformation of the helix structure to the ferromagnet at $x \rightarrow x_c$ at zero field. We concluded that this transformation is caused by different signs of the spin helicity for the compounds with $x > x_c$ and $x < x_c$. We believe that the mechanism of the transformation is caused by the competition between the Dzyaloshinskii-Moriya interaction and the cubic anisotropy.

DOI: [10.1103/PhysRevB.90.174414](https://doi.org/10.1103/PhysRevB.90.174414)

PACS number(s): 75.30.Cr, 75.50.Bb

I. INTRODUCTION

The magnetic properties of the compounds with the cubic B20 structure are nowadays the subject of intensive investigations. These compounds have a noncentrosymmetric crystallographic structure described by the $P2_13$ space group, which produces the chiral spin-spin Dzyaloshinskii-Moriya (DM) interaction [1]. The major ferromagnetic exchange interaction J together with the DM interaction D stabilize the helical (homochiral) structure in these systems below T_c . In accordance with the model proposed in Ref. [2] (Bak-Jensen model), these two interactions are balanced in the value of the helix wave vector $k_s = D/J$. The difference in energies between the ferromagnetic collinear and helical states can be experimentally measured by the critical magnetic field H_{c2} needed to transform the helix into the ferromagnet. According to Ref. [3], this energy difference is equal to $g\mu_B H_{c2} \approx Ak_s^2$, where $A = J/S$ is the spin wave stiffness and S is the ordered spin. The weak anisotropic exchange and/or cubic anisotropy fix the direction of the magnetic helix along the principal axes of the cubic symmetry. Upon application of the magnetic field the helix wave vector \mathbf{k} rotates toward the field axis at the field H_{c1} , which is the measure for the anisotropic interactions. Thus, the set experimental parameters k_s, H_{c1}, H_{c2} , and S describe completely the magnetic system of such compounds and allow one to estimate in some cases the values of the ferromagnetic exchange interaction J and the DM interaction D .

There are numerous experiments confirming that the sense of the structural chirality (left or right) Γ_c determines rigorously the sense of the magnetic chirality γ_m [4–9]. However, the relation between two chiralities is found to be different for various B20 compounds. For Mn based compounds ($\text{Mn}_{1-x}\text{Fe}_x\text{Si}$ and $\text{Mn}_{1-x}\text{Co}_x\text{Si}$) the crystalline and magnetic chiralities have the same sense, while the chiralities Γ_c and

γ_m are opposite of each other for Fe based ones, i.e., for $\text{Fe}_{1-x}\text{Co}_x\text{Si}$ at $x \leq 0.5$.

The experimental evidence was recently given for the magnetic transition in the $\text{Mn}_{1-x}\text{Fe}_x\text{Ge}$ compounds, where the helix chirality can be altered by mixing the two types of the magnetic atoms (Fe and Mn) [10,11]. The left-handed helix observed for the compounds with $x < x_c$ transforms to the ferromagnetlike system with the wave vector $k_s \rightarrow 0$ at $x \rightarrow x_c = 0.75$ and becoming the right-handed helix for the compounds with $x > x_c$.

In this paper we report on another FeGe type of compounds ($\text{Fe}_{1-x}\text{Co}_x\text{Ge}$) showing the same phenomenon of the flip of spin chirality at the critical concentration x_c . We have found that the change of the chirality undergoes through the ferromagnetic state, characterized by the zero value of the wave vector $k = 0$ and lowering of the critical field H_{c2} to the value smaller than H_{c1} .

The manuscript is organized in the following way. Section II gives the magnetization measurements of the $\text{Fe}_{1-x}\text{Co}_x\text{Ge}$ compounds. The results of the experiments on the small angle neutron diffraction taken from these compounds are shown in Sec. III. Sections IV and V present discussion and conclusion, respectively.

II. MAGNETIZATION MEASUREMENTS

We have synthesized the whole range of $\text{Fe}_{1-x}\text{Co}_x\text{Ge}$ compounds with x running from 0.0 to 1.0. As they can only be synthesized under high pressure, samples are in a polycrystalline powder form with a crystallite size of order of 10 microns (see Ref. [12] for details). The x-ray powder diffraction confirmed the B20 structure of these samples. The pure compound FeGe is magnetically ordered in the spin spiral

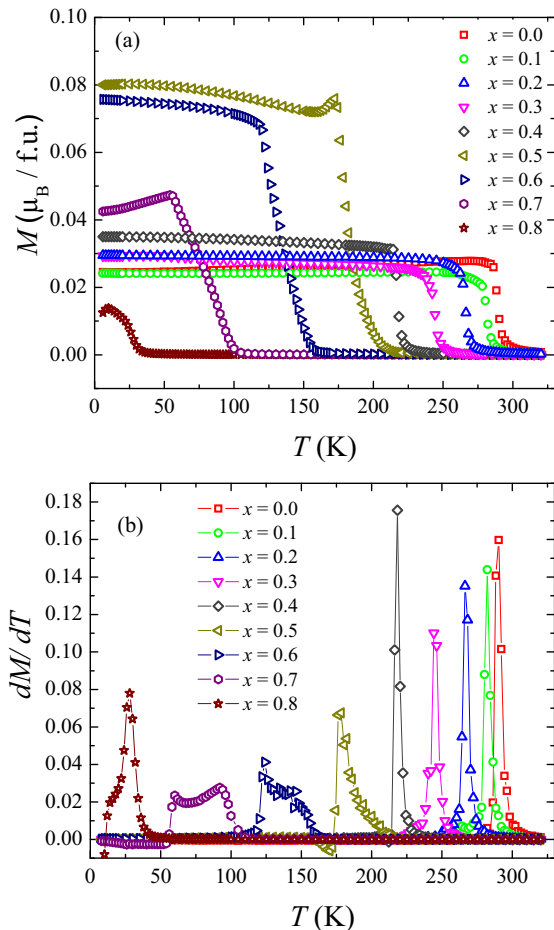


FIG. 1. (Color online) (a) The temperature dependence of the magnetization M for $\text{Fe}_{1-x}\text{Co}_x\text{Ge}$ compounds with $x = 0.0 \div 0.8$ at $H = 10$ mT. (b) The first derivative of the magnetization on the temperature dM/dT .

of Dzyaloshinskii type [13,14], while the pure CoGe is a Pauli paramagnet [15].

Magnetic measurements of newly synthesized compounds were carried out with the SQUID-magnetometer Quantum Design MPMS-5S, which is located at the Institute of Condensed Matter Physics, Braunschweig, Germany. Figure 1 gives the temperature scans of the magnetization for different compounds at the field $H = 10$ mT. The experimental curves from Fig. 1 allow one to estimate the ordering temperatures T_c . They were determined by taking the first derivative of the magnetization on the temperature dM/dT as the position of the sharp maxima of these derivatives on the temperature scale. However, the sharp maximum observed for the compounds with $x = 0.0 \div 0.5$ transforms into the two-feature dependence for the compounds with $x = 0.6$ and $x = 0.7$, showing the complexity of the magnetic phase transition of the compounds with these concentrations. We denote the high-temperature maximum as the ordering temperature for these compounds.

The magnetic field scans of the magnetization taken at low temperature are given in Fig. 2. The magnetization (in $\mu_B/f.u.$) increases linearly at small fields and saturates at H_{c2} , which is a characteristic field of transformation from

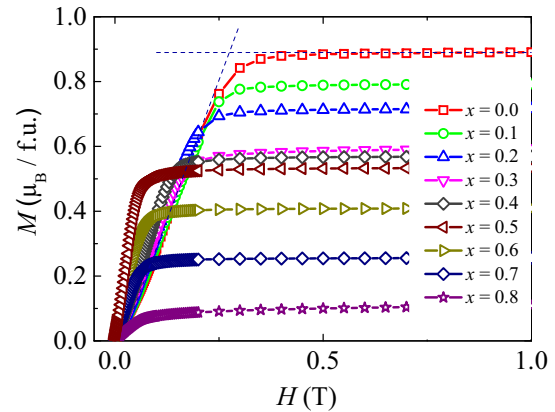


FIG. 2. (Color online) The magnetic field dependence of the magnetization M for $x = 0.0 \div 0.8$ at $T = 5$ K.

the conical (noncollinear) state to the ferromagnetic collinear one. The critical field is determined as the cross point of the linear approximations from the low-field and high-field ranges. Such dashed lines are shown only for the curve with $x = 0$ in Fig. 2.

The x dependence of the critical temperature T_c is shown in Fig. 3. T_c decreases monotonically on increase of x approaching 0 at $x \rightarrow 0.9$. The value of the ordered spin S per magnetic atom taken from SQUID measurements are also presented in Fig. 3 as a function of concentration x . As is seen in Figs. 2 and 3, S shows a little “shoulder” in the x dependence. These dependencies prove that the compounds are magnetically ordered below the critical temperature T_c in the wide range of the concentrations $x = [0.0 \div 0.8]$.

III. SMALL-ANGLE NEUTRON DIFFRACTION MEASUREMENTS

The magnetic structure of the samples was studied by the small-angle neutron scattering. The experiments were carried out at the setup SANS-1 at the Meier-Leibniz-Zentrum in Garching (Munich, Germany). The wavelength of the neutron beam was tuned from $\lambda = 0.5$ nm to 1.7 nm, and the beam

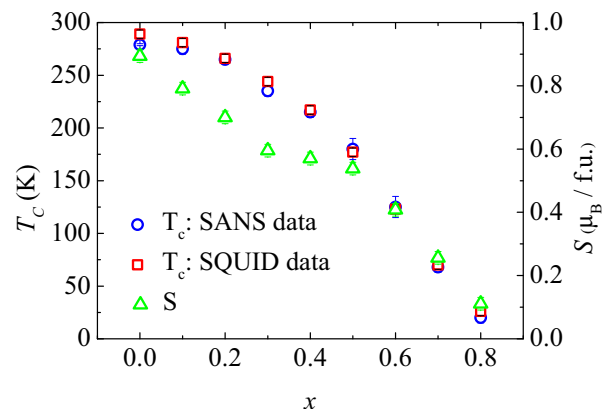


FIG. 3. (Color online) Dependence of the critical temperature T_c and the ordered spin value S on the concentration x of $\text{Fe}_{1-x}\text{Co}_x\text{Ge}$ compounds.

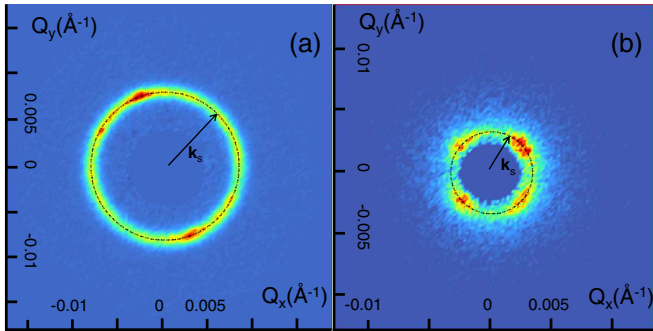


FIG. 4. (Color online) The small angle neutron scattering maps for the compounds with $x = 0.1$ (a) and 0.5 (b) at $T \approx 10$ K.

divergence was tuned from 0.5 mrad to 5 mrad to set the Q range and Q resolution optimal for an individual sample. The scattered neutrons were detected with a position sensitive detector with 128×128 pixels and a spatial resolution of 8 nm. With these settings we were able to cover the Q range from 2×10^{-2} to 1 nm $^{-1}$. The magnetic field up to 0.5 T was applied perpendicularly to the neutron beam. The temperature was set in the range from 10 to 300 K with accuracy of the order of 0.1 K.

Figure 4 shows examples of the small angle neutron scattering maps for the compounds with $x = 0.1$ and $x = 0.5$ at low temperatures. The SANS maps exhibit a ring corresponding to the scattering from randomly oriented spiral domains with the same helix wave vector $|\mathbf{k}_s|$. The scattering profiles were obtained from the SANS maps by circular averaging. The momentum transfer dependence of the scattering intensity $I(Q)$ is shown in Fig. 5. In order to better visualize a change of the peak position k_s , we plotted the argument Q in a logarithmic scale. As for the sample with $x = 0.6$ we have not observed any Bragg peak but only a tail of the diffuse scattering centered at $Q = 0$ as it is expected for ferromagnets.

Figure 6 shows the x dependence of the helix wave vector k_s . In the Fe-rich compounds k_s decreases for $x \in [0 \div 0.5]$, then it falls down to zero at $x \approx 0.6$, and increases again up to the value of $k_s = 0.14$ nm $^{-1}$ for the compound with

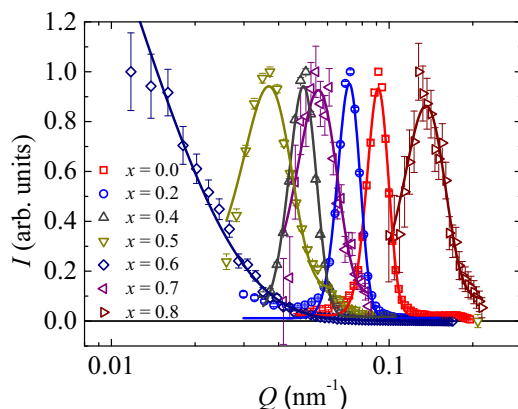


FIG. 5. (Color online) Momentum transfer dependence of the SANS intensity (normalized) at $T \approx 10$ K for compounds with $x = 0.0 \div 0.8$. The lines are the Gaussian fits.

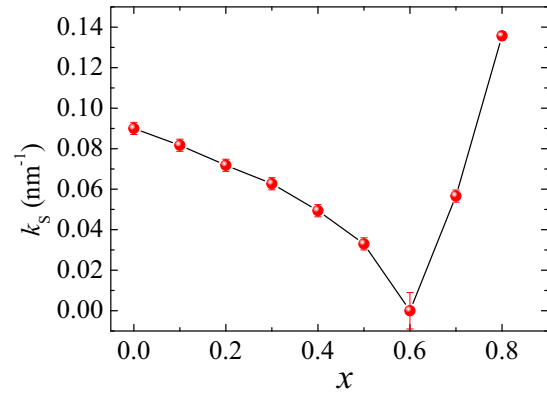


FIG. 6. (Color online) Dependence of the helix wave vector k_s on the concentration x .

$x = 0.8$. Accounting for the fact that the value of k_s approaches zero at $x_c \approx 0.6$ and the ordering temperature is as high as $T_c = 130$ K, we conclude that this compound is a ferromagnet, which is also in accordance with the Q dependence of the scattering intensity, shown in Fig. 5. This can only be possible if the macroscopic Dzyaloshinskii constant D is effectively vanishing.

In any case, the x dependence of the wave vector k_s in the Co-rich part of compounds (Fig. 6) can now be interpreted as a change of the sign of \mathbf{k} (or chirality) at $x \approx 0.6$. Since we have found for FeGe that the left-handed crystal is connected to the right-handed spin helices [10] then the opposite must hold for the compounds with concentrations larger than $x_c \approx 0.6$. Therefore, the left-handed crystals of CoGe should produce the left-handed spin helices, if it was magnetically ordered. We warn here that the sign of the Dzyaloshinskii constant was not measured in these experiments as it cannot be extracted from the polycrystalline samples. Nevertheless the change of the sign at $x \approx 0.6$ is very likely as the similar situation occurs in the case of the $\text{Mn}_{1-x}\text{Fe}_x\text{Ge}$ compounds, where alteration of the chirality was detected at $x \approx 0.75$ [10,11].

As is mentioned in the introduction, the difference in energy between the ferromagnetic collinear and helical state is measured by the critical magnetic field H_{c2} needed to transform the helix into the ferromagnet. It is therefore instructive to follow the evolution of the magnetic structure of the $\text{Fe}_{1-x}\text{Co}_x\text{Ge}$ compounds under applied magnetic field. Figure 7 illustrates how the field affects the neutron scattering intensity for the compound with $x = 0.0$ at low temperatures, while Fig. 8 represents the integral intensity I at $\mathbf{Q} \parallel \mathbf{H}$ as a function of the field. When the sample is cooled in zero field, scattering intensity is formed as a ring coming from the randomly oriented spirals of different crystallites [Fig. 7(a)]. At zero field the integral intensity is rather low, since the scattering is almost homogeneously distributed over the sphere with radius $Q = k_s$. The scattering intensity does not change at low field $H < H_{c1}$, since a weak field is not able to change the helix domain structure with the random orientation of \mathbf{k}_s fixed by the anisotropic exchange interaction and/or cubic anisotropy. The integral intensity increases upon increase of the field above H_{c1} , showing the process of the reorientation from the multidomain to the single domain structure [Fig. 7(b)]. The

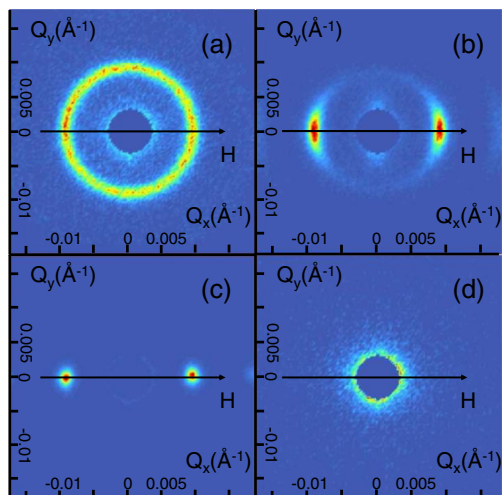


FIG. 7. (Color online) The small angle neutron scattering maps for the compound with $x = 0.0$ and (a) $H = 0.01$ T, (b) $H = 0.1$ T, (c) $H = 0.25$ T, (d) $H = 0.5$ T at $T \approx 10$ K.

ring of the intensity transforms smoothly into spots laying on the field axis [Fig. 7(c)]. With further increase of the field the reflections vanish at the second critical field H_{c2} , where the sample transforms into the ferromagnetic state [Fig. 7(d)].

The field H_{c2} is determined as the cross point of the linear approximation of the experimental curves and the H axis. The dashed lines in Fig. 8 illustrate the corresponding linear approximations. The critical field H_{c1} also can be estimated from the low field range of these curves as the field where the intensity starts to grow. It corresponds to the very beginning of the transformation of the ring in Fig. 7(a) into the two spots well smeared along the ring in Fig. 7(b).

We plot the critical fields H_{c1} and H_{c2} in dependence on the concentration x in Fig. 9. It is known that both H_{c1} and H_{c2} depend on the orientation of the magnetic field with respect to the crystallographic axis. As we have dealt with the powder samples, then both the critical fields H_{c1} and H_{c2} in our measurements are averaged over the possible directions

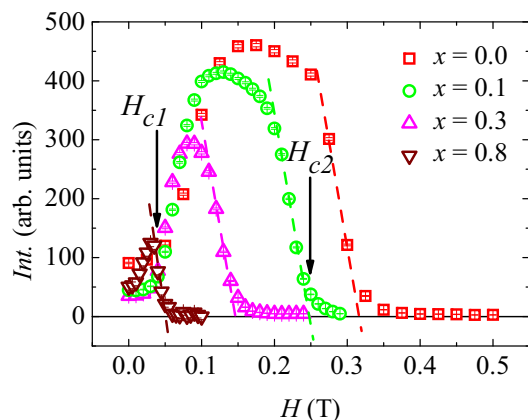


FIG. 8. (Color online) Magnetic field dependence of the integral intensity of the peak at $T = 10$ K for the compounds with $x = 0.0, 0.1, 0.3, 0.8$. The arrows correspond to the critical fields H_{c1} and H_{c2} for $x = 0.1$.

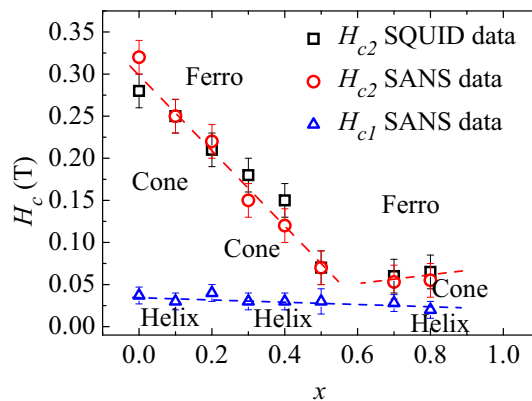


FIG. 9. (Color online) Dependence of the critical field H_{c1} and H_{c2} on the concentration x .

in the crystal. Nevertheless the values of the critical field H_{c2} obtained from the magnetization measurements (Fig. 2) coincide with those obtained in the SANS measurements (Fig. 8) within the error bars. This gives an additional confidence to the values extracted from the data.

The field H_{c1} changes little with the concentration x and is roughly equal to 0.03 T. Similarly to the x dependence of the wave vector k_s (Fig. 6), the critical field H_{c2} decreases linearly from $x = 0$ to $x = 0.6$. Then it shows a tendency for an increase at $x = 0.7$ and 0.8 . Figure 9 represents the $H - x$ phase diagram of the $\text{Fe}_{1-x}\text{Co}_x\text{Ge}$ compounds. The magnetic system is ordered in the plane spin helix below the critical field H_{c1} . It is transformed into the cone structure with the wave vector \mathbf{k} along the field axis in the range of fields between H_{c1} and H_{c2} . It becomes the ferromagnet with the spins aligned along the field axis at the field above H_{c2} .

The three states of the magnetic system (helix, cone, and ferromagnet) are separated by the critical fields H_{c1} and H_{c2} , respectively. In the vast variety of the B20 compounds the field H_{c1} is much smaller than H_{c2} . It is, for example, fulfilled for the pure FeGe ($x = 0$). However, as the concentration x approaches the value 0.6 the field H_{c2} becomes small and comparable to the field H_{c1} . These experimental data show that the magnetically ordered B20 compound becomes ferromagnetic when the energy difference between helical and ferromagnetic structures measured by H_{c2} becomes smaller than the energy of the anisotropy.

The phenomenological Bak-Jensen model [2] resulting in the helix spin structure is built on the hierarchy of interactions: ferromagnetic exchange interaction, antisymmetric Dzyaloshinskii-Moriya interaction, and the anisotropic exchange interaction. Note that the anisotropic exchange interaction, being part of the exchange interaction, can not impose any limitation on the values of k_s and H_{c2} , which can go infinitively small. On the contrary, the cubic anisotropy was not initially included in the Bak-Jensen model, nevertheless, it can play an important role in cases when the value of the helix wave vector k_s becomes relatively small. The limitations related to the cubic anisotropy were discussed in Refs. [16] and [17], where the energy of the spin helix was compared to the energy of the domain walls in the ferromagnet. The two energies of the DMI and the cubic anisotropy can be directly compared in the

Bak-Jensen model if one neglects the anisotropic exchange but includes the cubic anisotropy [3]. It can be shown that the cubic anisotropy, firstly, leads to the conditions limiting the stability of the helix phase in the range of small k_s and, secondly, makes its own contribution to the value of the critical field H_{c2} [18]. However, the interplay between the anisotropic exchange interaction and the cubic anisotropy for the different crystal orientations can considerably complicate the situation around $x \sim x_c$.

IV. CONCLUSION

To summarize, we observe a transformation of the helix structure to the ferromagnet at $x \rightarrow x_c$. We concluded that this transformation is caused by different signs of the spin helicity for the compounds with $x > x_c$ and $x < x_c$. The mechanism of the transformation can be realized via the competition between the Dzyaloshinskii-Moriya interaction and the cubic anisotropy, i.e., the transformation occurs when H_{c2} becomes comparable to H_{c1} .

We consider these findings in the light of the hypothesis that the sign of the effective macroscopic constant of the DM interaction depends on a 3d element occupying metal site. This hypothesis was formulated in Ref. [10] on the basis of observations concerning the monosilicides and monogermanides of the Mn and Fe based compounds. The hypothesis has a strong predictive power. Using this hypothesis one is able to predict that DM interaction should go to zero at a certain concentration x in compounds with two 3d element occupying metal sites, provided that these elements give different signs of DM interaction for the pure compounds.

Similarly to the $\text{Fe}_{1-x}\text{Co}_x\text{Ge}$ compounds studied here and according to hypothesis, the Fe-based silicides *should* have the opposite chirality as compared to the Co-based silicides. Therefore, firstly, the $\text{Fe}_{1-x}\text{Co}_x\text{Si}$ compounds should have the chirality flip upon change of the concentration in the range of $x = 0.6-0.7$. Secondly, the $\text{Mn}_{1-x}\text{Co}_x\text{Ge}$ compounds *should not* have the chirality flip upon change of the concentration since Mn-based germanides/silicides have chirality similar to the Co-based germanides. The neutron scattering experiments can prove the hypothesis in the nearest future. This hypothesis formulated in Ref. [10] can be considered in terms of the electron concentration dependence of the DM interaction as the d-band is filled [19]. This work [19] gives an interesting aspect of the problem, but the physics of these B20 systems appears to be more complex.

Generalizing the conclusion, we have demonstrated that the change of magnetic chirality is genetic property of the mixed compounds $\text{T1}_{1-x}\text{T2}_x\text{Ge}$ (where T1 and T2 are the transition metals). The Mn-, Co-, and Fe-based B20 compounds possess different signs of the DM interaction for the crystals of the same chirality and, thus, produce helices of the different chiralities.

ACKNOWLEDGMENTS

The authors are grateful to S.M. Stishov and S.V. Maleyev for useful discussions. The work was supported by the Russian Foundation for Basic Research (Grant Nos. 13-02-01468, 14-22-01073, and 14-02-00001) and by special programs of the Department of Physical Science, Russian Academy of Sciences.

-
- [1] I. E. Dzyaloshinskii, Zh. Eksp. Teor. Fiz. **46**, 1420 (1964) [Sov. Phys. JETP **19**, 960 (1964)].
- [2] P. Bak and M. H. Jensen, J. Phys. C **13**, L881 (1980).
- [3] S. V. Maleyev, Phys. Rev. B **73**, 174402 (2006).
- [4] M. Tanaka, H. Takayoshi, M. Ishida, and Ya. Endoh, J. Phys. Soc. J. **54**, 2970 (1985).
- [5] M. Ishida, Ya. Endoh, S. Mitsuda, Yo. Ishikawa, and M. Tanaka, J. Phys. Soc. J. **54**, 2975 (1985).
- [6] S. V. Grigoriev, D. Chernyshov, V. A. Dyadkin, V. Dmitriev, S. V. Maleyev, E. V. Moskvina, D. Menzel, J. Schoenes, and H. Eckerlebe, Phys. Rev. Lett. **102**, 037204 (2009).
- [7] S. V. Grigoriev, D. Chernyshov, V. A. Dyadkin, V. Dmitriev, E. V. Moskvina, D. Lamago, Th. Wolf, D. Menzel, J. Schoenes, S. V. Maleyev, and H. Eckerlebe, Phys. Rev. B **81**, 012408 (2010).
- [8] V. A. Dyadkin, S. V. Grigoriev, D. Menzel, D. Chernyshov, V. Dmitriev, J. Schoenes, S. V. Maleyev, E. V. Moskvina, and H. Eckerlebe, Phys. Rev. B **84**, 014435 (2011).
- [9] D. Morikawa, K. Shibata, N. Kanazawa, X. Z. Yu, and Y. Tokura, Phys. Rev. B **88**, 024408 (2013).
- [10] S. V. Grigoriev, N. M. Potapova, S.-A. Siegfried, V. A. Dyadkin, E. V. Moskvina, V. Dmitriev, D. Menzel, C. D. Dewhurst, D. Chernyshov, R. A. Sadykov, L. N. Fomicheva, and A. V. Tsvyashchenko, Phys. Rev. Lett. **110**, 207201 (2013).
- [11] K. Shibata, X. Z. Yu, T. Hara, D. Morikawa, N. Kanazawa, K. Kimoto, S. Ishiwata, Y. Matsui, and Y. Tokura, Nat. Nanotechnol. **8**, 723 (2013).
- [12] A. Tsvyashchenko, J. Less Common Metals **99**, L9 (1984).
- [13] B. Lebech, J. Bernhard, and T. Freltoft, J. Phys. Condens. Matter **1**, 6105 (1989).
- [14] E. Moskvina, S. Grigoriev, V. Dyadkin, H. Eckerlebe, M. Baenitz, M. Schmidt, and H. Wilhelm, Phys. Rev. Lett. **110**, 077207 (2013).
- [15] A. V. Tsvyashchenko, V. A. Sidorov, L. N. Fomicheva, V. N. Krasnorussky, R. A. Sadykov, J. D. Thompson, K. Gofryk, F. Ronning, and V. Yu. Ivanov, Solid State Phenomena **190**, 225 (2012).
- [16] A. N. Bogdanov and D. A. Yablonsky, Zh. Eksp. Teor. Fiz. **95**, 178 (1989) [Sov. Phys. JETP **68**, 101 (1989)].
- [17] A. N. Bogdanov, U. K. Roessler, and C. Pfleiderer, Physica B **359**, 1162 (2005).
- [18] S. V. Maleyev (private communication).
- [19] E. W. Achi, H. J. Al-Kanani, J. G. Booth, M. M. R. Costa, and B. Lebech, J. Magn. Magn. Mater. **177-181**, 779 (1998).